

Alendronate promotes bone formation by inhibiting protein prenylation in osteoblasts in rat tooth replantation model

Koichiro Komatsu¹, Akemi Shimada¹, Tatsuya Shibata¹, Satoshi Wada², Hisashi Ideno^{1,3}, Kazuhisa Nakashima¹, Norio Amizuka⁴, Masaki Noda⁵ and Akira Nifuji^{1,3}

Departments of ¹Pharmacology and ²Orthodontics, School of Dental Medicine, Tsurumi University, 2-1-3 Tsurumi, Tsurumi-ku, Yokohama 230-8501, Japan

³Transcriptome Research Group, National Institute of Radiological Sciences, 4-9-1 Anagawa, Inage-ku, Chiba 263-8555, Japan

⁴Department of Developmental Biology of Hard Tissue, Graduate School of Dental Medicine, Hokkaido University, Kita 13, Nishi 7, Kita-ku, Sapporo 060-8586, Japan

⁵Department of Molecular Pharmacology, Medical Research Institute, Tokyo Medical and Dental University, 1-5-45 Yushima, Chiyoda-ku, Tokyo 113-8510, Japan

Correspondence should be addressed to K Komatsu or A Nifuji
Email
komatsu-k@tsurumi-u.ac.jp or nifuji-a@tsurumi-u.ac.jp

Abstract

Bisphosphonates (BPs) are a major class of antiresorptive drug, and their molecular mechanisms of antiresorptive action have been extensively studied. Recent studies have suggested that BPs target bone-forming cells as well as bone-resorbing cells. We previously demonstrated that local application of a nitrogen-containing BP (N-BP), alendronate (ALN), for a short period of time increased bone tissue in a rat tooth replantation model. Here, we investigated cellular mechanisms of bone formation by ALN. Bone histomorphometry confirmed that bone formation was increased by local application of ALN. ALN increased proliferation of bone-forming cells residing on the bone surface, whereas it suppressed the number of tartrate-resistant acid phosphatase (TRAP)-positive osteoclasts *in vivo*. Moreover, ALN treatment induced more alkaline phosphatase-positive and osteocalcin-positive cells on the bone surface than PBS treatment. *In vitro* studies revealed that pulse treatment with ALN promoted osteocalcin expression. To track the target cells of N-BPs, we applied fluorescence-labeled ALN (F-ALN) *in vivo* and *in vitro*. F-ALN was taken into bone-forming cells both *in vivo* and *in vitro*. This intracellular uptake was inhibited by endocytosis inhibitors. Furthermore, the endocytosis inhibitor dansylcadaverine (DC) suppressed ALN-stimulated osteoblastic differentiation *in vitro* and it suppressed the increase in alkaline phosphatase-positive bone-forming cells and subsequent bone formation *in vivo*. DC also blocked the inhibition of Rap1A prenylation by ALN in the osteoblastic cells. These data suggest that local application of ALN promotes bone formation by stimulating proliferation and differentiation of bone-forming cells as well as inhibiting osteoclast function. These effects may occur through endocytic incorporation of ALN and subsequent inhibition of protein prenylation.

Key Words

- ▶ bone formation and resorption
- ▶ skeletal biology
- ▶ osteoblast
- ▶ histology

Journal of Endocrinology
(2013) 219, 145–158

Introduction

Bisphosphonates (BPs) are a major class of antiresorptive drug. BPs are divided into nitrogen-containing BPs (N-BPs) and non-N-BPs. The P–C–P backbone structure of BPs exhibits a high affinity for bone mineral, and therefore BPs accumulate on bone surfaces (Sato *et al.* 1991, Azuma *et al.* 1995, Masarachia *et al.* 1996). Osteoclasts internalize accumulated BPs during the bone resorption process (Thompson *et al.* 2006, Coxon *et al.* 2008, Roelofs *et al.* 2010). Interestingly, uptake of fluorescence-labeled BPs such as alendronate (ALN) and risedronate by phagocytic cells was observed *in vitro* and *in vivo*, and was inhibited by endocytosis inhibitors *in vitro* (Thompson *et al.* 2006, Roelofs *et al.* 2010), suggesting that cellular uptake of BPs is a prerequisite for their effects on osteoclastic bone resorption.

Molecular analysis of their effect on bone resorption revealed that N-BPs such as ALN, risedronate, and zoledronate inhibit farnesyl diphosphate synthase, a key enzyme of the mevalonate pathway. They subsequently prevent the synthesis of isoprenoids required for prenylation of small GTPases such as Rap, Rac, Rho, Rab, and Cdc42. Accumulation of unprenylated small GTPases by N-BPs causes disruption of the actin cytoskeleton, altered trafficking of intracellular components, and impaired integrin signaling in osteoclasts (Luckman *et al.* 1998, Dunford *et al.* 2006, Rogers *et al.* 2011).

N-BPs may also target other cell types such as bone-forming cells. N-BPs stimulate proliferation and differentiation of osteoblasts at low concentrations. At high concentrations, N-BPs inhibit proliferation and bone nodule formation (Giuliani *et al.* 1998, Reinholtz *et al.* 2000). It has also been pointed out that higher concentrations of N-BPs are likely to be necessary for intracellular inhibition of small GTPase prenylation in osteoblasts (Coxon *et al.* 2008, Idris *et al.* 2008) and the antiapoptotic effects of N-BPs at low concentrations on osteoblasts may be exerted through activation of ERKs (Bellido & Plotkin 2011).

Local application of N-BPs has been shown to promote bone formation around N-BP-coated implants *in vivo* (Tanzer *et al.* 2005, Gao *et al.* 2009). Previously, we reported that bone tissues were increased around replanted teeth to which ALN was locally applied for a short duration of time (Shibata *et al.* 2004, Komatsu *et al.* 2008). Thus far, however, the precise biological mechanisms of this anabolic action on bone have remained unclear.

In this study, we extended our previous research to investigate the mechanisms of bone formation by local application of ALN. We adopted two approaches,

histochemical analysis of an *in vivo* tooth replantation model and cellular analysis using *in vitro* primary osteoblastic cells, with a particular focus on intracellular ALN uptake into cells. We found that ALN affects proliferation and differentiation of osteoblasts as well as osteoclast function, and these effects possibly occur through endocytic intracellular uptake of ALN into those cells.

Materials and methods

All animal studies were approved by the Animal Care Committee of Tsurumi University School of Dental Medicine.

Local application of ALN in tooth replantation model

To assess local effects of N-BPs on bone remodeling, a tooth replantation model (Shibata *et al.* 2004) was used (Supplementary Figure 1, see section on supplementary data at the end of this article). Briefly, rat molars were extracted, immersed in 1 mM ALN (ALN group, $n=35$) or PBS alone (PBS group, $n=28$) for 5 min at room temperature, and put back into their sockets under anesthesia. In normal control rats (nonRL group, $n=22$), the teeth were not extracted. For local application of ALN with endocytosis inhibitor dansylcadaverine (Haigler *et al.* 1980, Thompson *et al.* 2006, Chen *et al.* 2009) (DC, a clathrin-mediated endocytosis inhibitor), extracted teeth were immersed in PBS ($n=4$), 1 mM ALN ($n=4$), 1 mM ALN+1 mM DC ($n=4$), and 1 mM DC ($n=4$) for 5 min at room temperature, and put back into their sockets. At certain time points, tissues were fixed and subjected to bone histomorphometry and immunohistochemistry (see below).

Bone histomorphometry Animals in the ALN ($n=6$), PBS ($n=5$), and nonRL ($n=4$) groups received s.c. injections of calcein (5 mg/kg) on day 2 after tooth replantation and of Alizarin red (15 mg/kg) on day 16. Undecalcified sections were prepared (Schenk *et al.* 1984) from maxillae dissected on day 18, and observed with a confocal laser scanning microscope (CLSM, PCM2000, Nikon, Tokyo, Japan). We used CLSM images for bone histomorphometry (Parfitt *et al.* 1987). The whole interradicular area between the mesial and distal roots (tissue volume (TV) (mm^2); Fig. 1A, upper panel) was measured by manually tracing the boundaries between tooth root surfaces or bone surfaces and soft tissues on histological sections using Image J (NIMH, Bethesda, MD, USA). The area of bone (bone volume (BV) (mm^2)) within the TV was

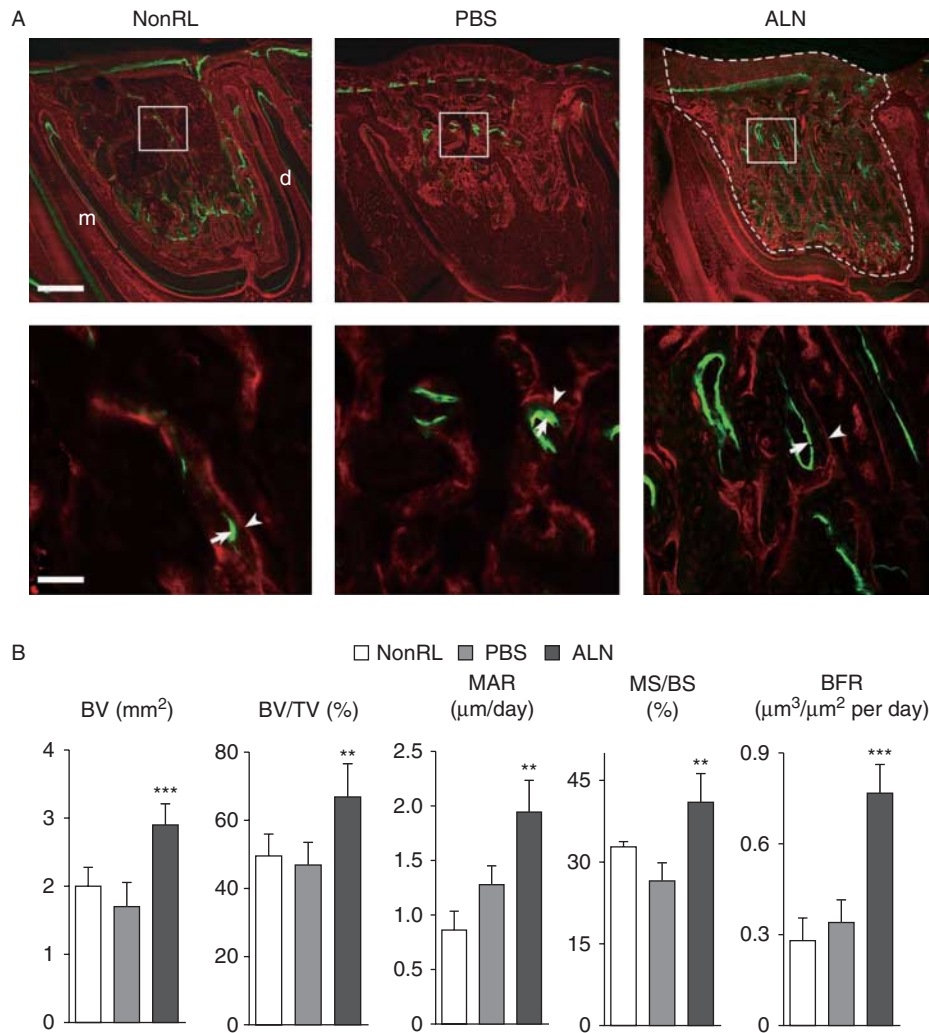


Figure 1

Local ALN treatment accelerates bone formation *in vivo*. (A) Confocal laser scanning microscopy of undecalcified longitudinal sections of rat maxillary first molars 18 days after replantation. The teeth were replanted after pretreatment with PBS (middle column) or 1 mM alendronate (ALN, right column). Sections were also prepared from nonreplanted teeth (nonRL, left column). (Lower panels) Magnified images of white squares in the upper panels showing double bone labels by Alizarin red (arrowheads) and calcein (arrows). m, mesial root; d, distal root. Scale bars for upper panel, 0.5 mm and for lower panel, 100 µm. (B) Bone histomorphometry.

measured by manually tracing the boundaries between the bone surfaces and soft tissues using Image J. BV/TV was then calculated. In addition, mineral apposition rate (MAR (µm/day)) was measured as the distance between two consecutive labels (Fig. 1A, lower panel) divided by 14 days. Mineralizing surface per bone surface (MS/BS (%)) was measured as $100 \times (\text{double label surface} + 0.5 \times \text{single label surface}) / \text{bone surface}$ (Parfitt *et al.* 1987) in selected areas (0.65 × 0.65 mm), for trabecular bones of the inter-radicular region between the mesial and distal roots

Bone volume (BV (mm²)) and bone volume/tissue volume (BV/TV (%)) were determined within the area (TV) surrounded by the white dotted line in (A). Mineral apposition rate (MAR (µm/day)) was determined from the distance, as indicated by white arrows, between two consecutive labels and mineralizing surface per bone surface (MS/BS (%)) for trabecular bones of the inter-radicular region between the mesial and distal roots. Then, bone formation rate (BFR) was determined as product of MAR and MS/BS. Each column and bar indicate mean + 1 s.d. Significant differences from the PBS group: ** $P < 0.01$ and *** $P < 0.001$.

using Image J. Then, bone formation rate (BFR) was determined as product of MAR and MS/BS/100.

Procedures of immunohistochemistry for BrdU and osteocalcin, and of tartrate-resistant acid phosphatase (TRAP) and alkaline phosphatase (ALP) staining

Local application of a fluorescence-labeled ALN analog in replanted teeth To track the target cells of

ALN after tooth replantation, a fluorescence-labeled analog of ALN (F-ALN) was prepared by covalent conjugation of ALN to N-hydroxysuccinimide-5-(and 6-)-carboxy-fluorescein (Pierce, Rockford, IL, USA; Zaheer *et al.* 2001, Thompson *et al.* 2006; Supplementary Methods, see section on supplementary data at the end of this article). To determine the ratio of labeled ALN:non-labeled ALN in the prepared solution, we measured the absorbance at 494 nm. The concentration of F-ALN was calculated to be 1.1 mM. Different mobilities of the F-ALN and of the fluorescence probe by thin layer chromatography (TLC) were confirmed (Zaheer *et al.* 2001). The mobile phase was 32.5% acetonitrile/67.5% H₂O. Non-labeled ALN was detected with 0.25% ninhydrin in acetone and heat (110 °C) on TLC plate, and the concentration of non-labeled ALN in the F-ALN solution was estimated to be 3.1 mM. Thus, the F-ALN solution prepared in our laboratory contained 26% labeled ALN and 74% free ALN.

Extracted teeth were immersed in 1 mM F-ALN (F-ALN group), 1 mM non-labeled ALN (ALN group), or 1 mM fluorescein for 5 min at room temperature, and put back into their sockets. In normal control rats (nonRL group), the teeth were not extracted. On days 1, 4, 7, and 56, the maxillae were dissected. Supplementary Table 1, see section on supplementary data at the end of this article, shows the allocated numbers of rats used for experiments to investigate localization of F-ALN. Undecalcified sections were prepared (Schenk *et al.* 1984) and examined with a fluorescence microscope (ECLIPSE E800 or 80i, Nikon). Some sections were counterstained with DAPI. Fluorescence microscopic images were taken under the same exposure times.

Culture of primary rat calvarial osteoblasts and ROS 17/2.8 cell line

Primary osteoblastic cells were isolated from calvariae of newborn rats by serial enzymatic digestion (Wada *et al.* 1998). Cells were cultured in α -MEM (growth medium) containing 10% FCS and antibiotics (100 IU/ml penicillin G and 100 μ g/ml streptomycin). Cells at the second passage were used for experiments. To differentiate osteoblasts, 5 mM β -glycerophosphate and 50 μ g/ml ascorbic acid with

or without 10⁻⁸ M dexamethasone were added to growth medium (differentiation medium). The osteoblast-like cell line ROS 17/2.8 was maintained in F-12 medium containing 5% FCS. Cell culture dishes were incubated in a humidified atmosphere of 5% CO₂ in air at 37 °C. The medium was changed every 2 or 3 days.

Methyl thiazolyl tetrazolium (MTT) assay Cells were plated in 96-well plates at 5 × 10³ cells/well and cultured for 2 days (until subconfluence) in growth medium. On day 2, the medium was replaced with differentiation medium. On day 3, ALN was added to the medium at 10⁻⁶ or 10⁻⁵ M in the presence or absence of 100 μ M DC or 20 μ M geranylgeraniol (GO). On day 6, the medium was replaced with fresh medium, and the culture continued. On days 7 and 14, MTT assay was performed.

Real-time RT-PCR analysis Cells (10⁵) were plated in six-well plates and treated as described for the MTT assay. On days 7 and 14, total RNA was extracted and real-time RT-PCR analysis was performed (Ideno *et al.* 2009). The primer sequences are listed in Table 1.

ALP activity assay and Alizarin red staining Cells (2 × 10⁴) were plated in 24-well plates and treated as described for the MTT assay. On days 7, 14, and 21, ALP activity assay and Alizarin red staining were performed (Ideno *et al.* 2009).

Cellular uptake of F-ALN Cells were plated onto glass coverslips and cultured in growth medium. We also prepared a fluorescently labeled analog of ALN (AX-ALN) by covalent conjugation of ALN to Alexa Fluor 488 carboxylic acid, succinimidyl ester (Molecular Probes, Eugene, OR, USA), in a procedure similar to that for F-ALN. The AX-ALN solution prepared in our laboratory contained 10% labeled ALN and 90% free ALN. Cells were incubated with AX-ALN or F-ALN (10⁻⁴, 10⁻⁵, and 10⁻⁶ M) in the presence or absence of 100 μ M DC and 20 μ M chlorpromazine (CP), a clathrin-mediated endocytosis inhibitor, or 1 mM methyl- β -cyclodextrin (MB), a caveolin-mediated endocytosis inhibitor (Thompson *et al.* 2006, Kelley *et al.* 2009, Masaike *et al.* 2010).

Table 1 Primers for real-time PCR experiments

	Accession numbers	Forward primers	Reverse primers
GAPDH	M32599	GCCAAACGGGTCATCATCTC	GTCATGAGCCCTTCCACAAT
ALP	NM_013059	GACAAGAAGCCCTTCACAGC	GGGGATGTAGTTCTGCTCA
Osteocalcin	NM_013414.1	CAAGCAGGAGGGCAGTAAGG	CCATAGATGCGCTTGTAGGC

After treatment for 1 and 4 h, the coverslip-bound cells were fixed in 3.7% formaldehyde, and examined in a CLSM (TCS-SP5, Leica, Tokyo, Japan). CLSM images were acquired under identical laser and detection values (Blue Diode 405 nm laser and Ar 488 nm laser, sequential scan mode, PL APO 63× oil immersion objective lens, image size 1024×1024 pixel, z-step size 0.5–0.6 μm, z volume 11–16 μm) by using LAS AF Software (Leica, Tokyo, Japan). Some cells were counterstained with DAPI.

Western blot analysis Cells (10^5) were plated in six-well plates and cultured in F-12 medium containing 5% FCS. After subconfluence, to examine the inhibition of protein prenylation by ALN, cells were starved in F-2 medium containing 0.1% BSA overnight, and then treated with 10^{-6} , 10^{-5} , or 10^{-4} M ALN for 24 h in the presence or absence of DC (100 μM) or GO (20 μM) for 24 h. To examine activation of ERK by ALN, cells were treated as described above and treated with ALN (10^{-6} or 10^{-5} M) for 3 or 10 min in the presence or absence of DC (100 μM), or bFGF (10 ng/ml) for 15 min as positive control. Cell lysates were subjected to 12% SDS-PAGE and immunoblot analyses using antibodies against Rap1A (1:300, sc-1482, Santa Cruz), which specifically recognizes the unprenylated form of Rap1A (Reszka *et al.* 2001, Thompson *et al.* 2006), Rap1 (1:300, sc-65, Santa Cruz), phosphorylated ERK1/2 (1:1000, sc-783, Santa Cruz), or total ERK1/2 (1:1000, sc-94, Santa Cruz). The immunoreactive protein bands were detected using HRP-conjugated secondary antibodies and chemiluminescence (Ideno *et al.* 2009).

Statistical analysis

For the tooth replantation model, data are shown as mean and s.d. of three to five rats. For cell culture, data are presented from a typical one of two or three repeated experiments and are shown as the mean and s.d. of two to five samples. Statistical differences were evaluated using ANOVA followed by *post hoc* Scheffé's test or *t*-test.

Results

Effects of local ALN treatment on bone formation

To examine whether locally applied ALN affects bone formation, we performed double-fluorochrome labeling. Double labels in the ALN group were observed in broad areas around the replanted teeth, and interlabel distances were wider than in the PBS and nonRL groups (white arrows in Fig. 1A, lower panels). BV and BV/TV were greater in the ALN group than in the nonRL and PBS

groups ($P < 0.01$ or 0.001 ; Fig. 1B). MAR, MS/BS, and BFR were also greater in the ALN group than in the PBS and nonRL groups ($P < 0.01$ or 0.001 ; Fig. 1B). These results indicate that bone formation was significantly accelerated in the trabecular bone around the replanted teeth in the ALN-treated group.

ALN inhibits TRAP-positive bone resorbing cells *in vivo*

The morphology, localization, and number of TRAP-positive, attached multinuclear cells remained similar in the PBS and ALN groups (Fig. 2) at 1 day after the operation. However, the number of TRAP-positive, attached multinuclear cells were significantly less in the ALN than in the PBS group at 4 and 7 days (Fig. 2). While large multinuclear TRAP-positive cells attached to active bone resorption sites in the PBS group, many TRAP-positive multinuclear cells in the ALN group were detached from resorption sites and demonstrated a round shape (Fig. 2), suggesting that they are less active. Thus, ALN inhibits TRAP-positive bone resorbing cell function *in vivo*.

ALN activates bone-forming cells *in vivo*

Since locally applied ALN stimulates bone formation, we examined effects of ALN on proliferation and differentiation of bone-forming cells *in vivo*. We analyzed proliferation by BrdU uptake and evaluated differentiation by ALP staining and osteocalcin. BrdU-positive cells were observed within the bone marrow and close to the bone surfaces (Fig. 3A). To count BrdU-positive bone-forming cells adjacent to bone surfaces, we measured them in the area within ± 24 μm from the bone surfaces. The number of BrdU-positive bone-forming cells was greater in the ALN group than the PBS group at days 1, 4, and 7 (Fig. 3B), although the difference was significant only at day 7 ($P < 0.05$). The ratio of ALP-positive cell surface:bone surface was significantly higher in the ALN group than in the PBS group at day 7 (Fig. 3C and D, $P < 0.05$). The ratio of osteocalcin-positive cell surface:bone surface was greater at days 4 and 7 in the ALN group than in the PBS group, although the difference was significant only at day 7 (Fig. 3E and F, $P < 0.01$). These results suggest that ALN promoted proliferation and differentiation of bone-forming cells *in vivo*.

The stimulating effect was only found for osteocalcin but not for ALP *in vitro*

We next examined the effects of ALN on proliferation and differentiation of bone-forming cells *in vitro*. The number

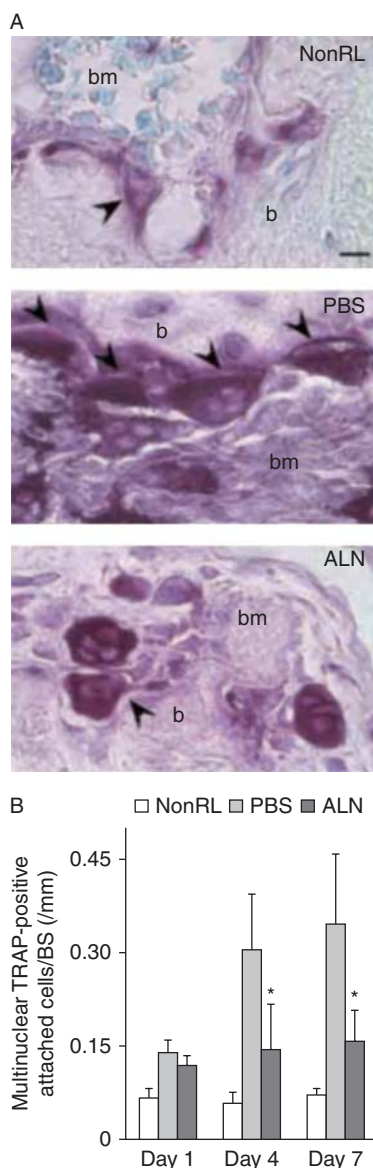


Figure 2

ALN inhibits tartrate-resistant acid phosphatase (TRAP)-positive bone resorbing cells *in vivo*. (A) TRAP staining 7 days after replantation showing characteristic morphologies of TRAP-positive cells. Pictures were taken from areas similar to those in the magnified images (lower panels) of Fig. 1A. Scale bar, 10 μ m. (B) Numbers of multinuclear TRAP-positive cells attached to trabecular bone surfaces (as indicated by arrowheads) between the mesial and distal roots of the replanted teeth 1, 4, and 7 days after replantation. Multinuclear TRAP-positive, attached cells are presented as number per bone surface (BS (mm)). b, bone; bm, bone marrow. Significant differences from the PBS group: * $P < 0.05$.

of primary osteoblastic cells markedly reduced after treatment with 10^{-4} M ALN for 3 days, but did not change after treatment with 10^{-5} – 10^{-8} M (Supplementary Figure 2A, see section on supplementary data at the end of this article). It has been reported that short-term

treatment (for 1–5 days) with 10^{-6} – 10^{-5} M zoledronic acid upregulates osteogenic gene expression (Chaplet *et al.* 2004, Pan *et al.* 2004). Therefore, we analyzed osteoblast differentiation *in vitro* after treatment with 10^{-5} and 10^{-6} M ALN for 3 days. ALN concentrations of 10^{-6} and 10^{-5} M did not affect cell viability (Supplementary Figure 2B), ALP gene expression, and ALP activity (Supplementary Figure 2C and D) at days 7 and 14. However, osteocalcin gene expression (Fig. 4A) and osteocalcin-positive cells (Fig. 4B and C) significantly increased at day 14 after treatment with 10^{-6} and 10^{-5} M ALN. Similar effects of ALN on osteocalcin gene expression were also observed when 10^{-8} M dexamethasone was added (Supplementary Figure 3).

F-ALN is taken into bone-forming cells *in vivo*

To determine the fate of locally applied ALN *in vivo*, we introduced F-ALN to visualize localization of ALN. Fluorescence microscopic analyses revealed extensive binding of F-ALN to mineralized surfaces of tooth roots of replanted teeth and their surrounding alveolar bones from days 1 through 56 after the operation (Supplementary Figure 4, see section on supplementary data given at the end of this article). We also observed binding of F-ALN to the trabecular bone surfaces of bone marrows distant from the replanted teeth (Supplementary Figure 4ii and iv) and around the replanted teeth (Supplementary Figure 4iii). Multinuclear cells residing around and distant from the replanted teeth incorporated large amounts of F-ALN at days 4 and 7 (Supplementary Figure 5). In addition to monocyte-lineage cells, bone-forming cells such as bone marrow stromal cells and osteoblast-like cells adjacent to the trabecular bone surfaces of bone marrows around (Fig. 5B, upper panels) and distant from (Fig. 5B, lower panels) the F-ALN-treated replanted teeth incorporated small amounts of F-ALN at days 1, 4, and 7. No fluorescence was detected in similar sites of non-labeled ALN-treated teeth (Fig. 5A, lower panel). These findings suggest that bone-forming cells or their progenitor cells directly incorporate ALN when ALN is applied locally *in vivo* even for a short period.

Cellular uptake of F-ALN by primary osteoblastic cells occurs through endocytosis

To examine the mechanism of ALN uptake by osteoblasts, primary osteoblastic cells were treated for 1 and 4 h with F-ALN in the presence or absence of endocytosis inhibitors. The concentrations of labeled ALN include

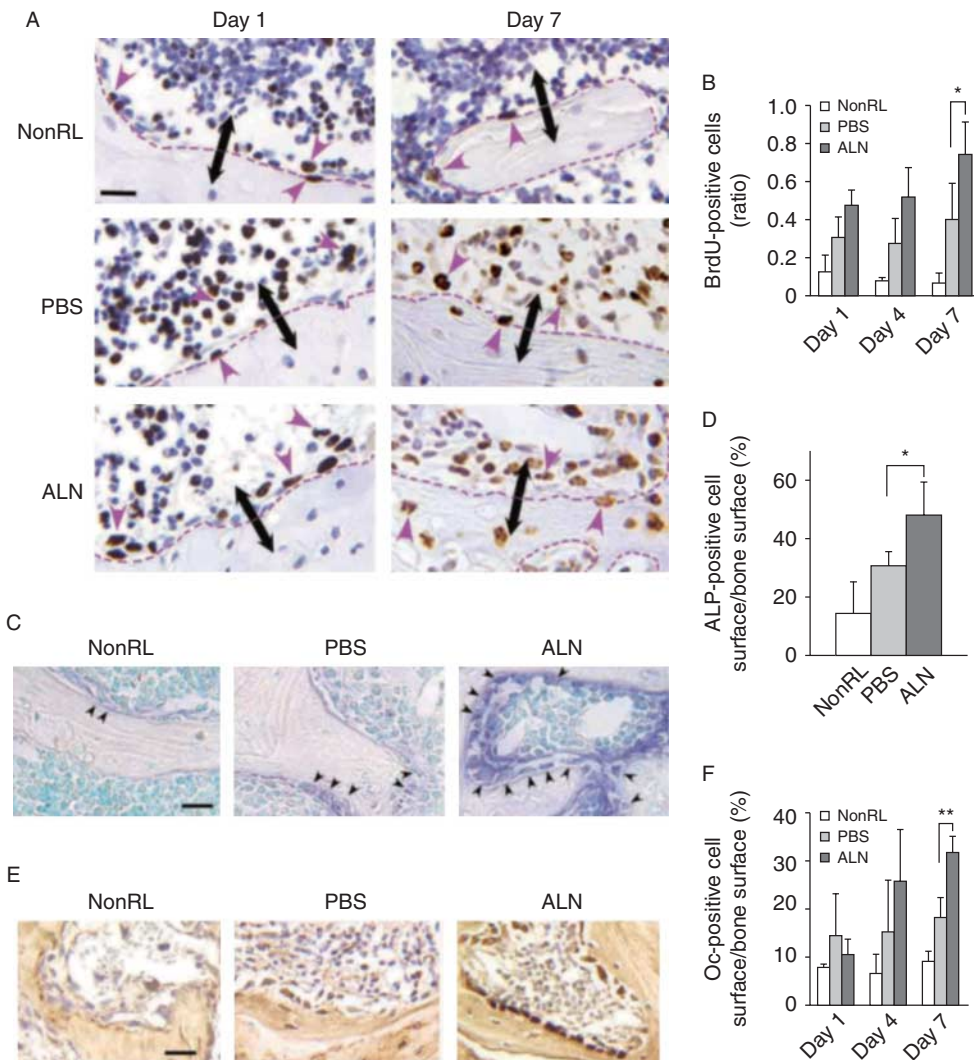


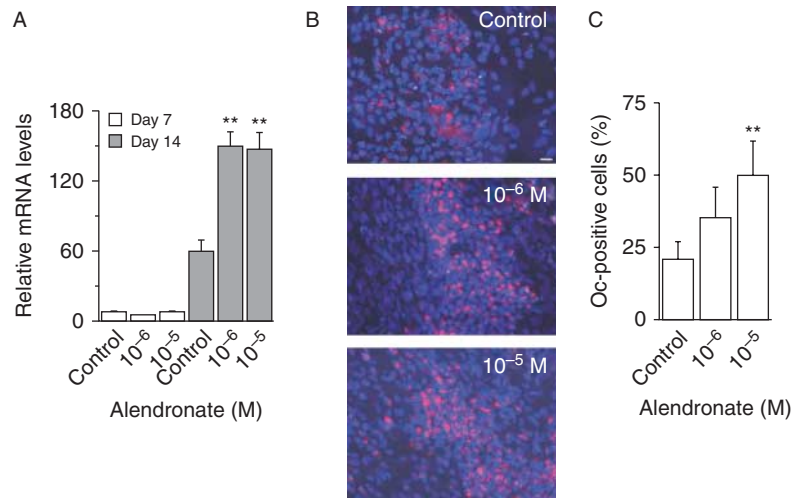
Figure 3

ALN activates bone-forming cells *in vivo*. (A) Immunostaining of BrdU-labeled cells between the mesial and distal roots of replanted teeth 2 h (day 1) and 6 days (day 7) after BrdU injection. Pictures were taken from areas similar to those in the magnified images (lower panels) of Fig. 1A. Arrowheads indicate BrdU-labeled cells in the area within $\pm 24 \mu\text{m}$ (as indicated by arrows) from bone surfaces (as traced by red dotted lines). Scale bar, $20 \mu\text{m}$. (B) Ratios of BrdU-positive cells in the area within $\pm 24 \mu\text{m}$ from bone surfaces including bone matrix. (C) Alkaline phosphatase (ALP)

staining 7 days after replantation. Pictures were taken from areas similar to those in (A). Arrowheads indicate ALP-positive cells. Scale bar, $20 \mu\text{m}$. (D) ALP-positive cell surface/bone surface (%). (E) Immunostaining for osteocalcin 7 days after replantation. Pictures were taken from areas similar to those in (A and C). Scale bar, $20 \mu\text{m}$. (F) Osteocalcin (Oc)-positive cell surface/bone surface (%). Each column and bar indicate mean ± 1 s.d. Significant differences from the PBS group: * $P < 0.05$ and ** $P < 0.01$.

the concentrations used to evaluate the effect on proliferation and differentiation in calvarial osteoblastic cells. Similar to *in vivo* results, osteoblastic cells incorporated F-ALN (Fig. 6A, upper panels) when incubated in 10^{-4} or 10^{-5} M AX-ALN and F-ALN in a dose-dependent manner, but we barely detected the intracellular incorporation at 10^{-6} M (not shown). Co-incubation with $100 \mu\text{M}$ DC or $20 \mu\text{M}$ CP, clathrin-mediated endocytosis inhibitors, considerably attenuated uptake of 10^{-5} M

(Fig. 6A, lower panels) and 10^{-4} M AX-ALN. A caveolin-mediated endocytosis inhibitor, MB (1 mM), did not markedly affect cellular uptake of AX-ALN. Vesicular localization of internalized labeled ALN closely resembled that of a fluorescence-labeled dextran analog, a general endocytosis marker (Supplementary Figure 6, see section on supplementary data given at the end of this article). These findings suggest that osteoblastic cells incorporate N-BPs through endocytosis.

**Figure 4**

Effect of ALN on osteoblast differentiation in primary rat calvarial osteoblastic cells. Cells were treated with 10^{-6} or 10^{-5} M ALN from day 3 to day 6. (A) Gene expression of osteocalcin (Oc). (B) Immunofluorescence staining of osteocalcin at day 14. After fixation, cells were incubated with anti-osteocalcin primary

antibody, stained with Alexa Fluor 594 conjugated secondary antibody (red) and counterstained with DAPI (blue). Scale bar, 30 μ m. (C) Ratio of osteocalcin-positive cells (%) on day 14. Each column + bar represents the mean + 1 s.d. Significant differences from the control: ** $P < 0.01$.

Endocytosis inhibition blocked ALN-enhanced osteoblastic differentiation *in vitro*

Since ALN uptake was mediated by endocytosis, one can assume that inhibition of endocytosis of ALN may inhibit ALN action on osteoblastic cells. We treated primary osteoblastic cells with ALN in the presence or absence of endocytosis inhibitor, DC. Mineralized area demonstrated a concentration-dependent increase at 21 days after treatment with ALN (Fig. 6B). The ALN-induced increase in mineralized area was cancelled by co-incubation with 100 μ M DC. The increases in osteocalcin gene expression and osteocalcin-positive cells were also blocked by DC (Supplementary Figure 7, see section on supplementary data at the end of this article). Thus, endocytosis inhibition blocked the ALN-stimulated osteoblast differentiation *in vitro*. Twenty micromoles GO, which restores geranylgeranylation (Dunford *et al.* 2006), also suppressed the increases in osteocalcin expression and osteocalcin-positive cells by ALN (Supplementary Figure 7).

Endocytosis inhibition blocked ALN-induced bone formation *in vivo*

To examine whether endocytic inhibition affects the ALN-induced bone formation *in vivo*, we added DC to the ALN solution, immersed extracted teeth in the solution, and then replanted them. More bone tissue was observed in ALN-treated tissue than in PBS-treated tissue on day 7

(Fig. 7A and B; $P < 0.01$). The addition of DC (1 mM) to the ALN solution significantly reduced the increase in the bone tissue induced by ALN pretreatment ($P < 0.05$). The addition of DC also reduced the ALN-induced increase in ALP-positive cell ratios (Fig. 7C and D; $P < 0.01$) and the ALN-induced decrease of attached TRAP-positive cells (Fig. 8A and B; $P < 0.05$). Thus, these results suggest that endocytosis inhibition cancelled the effects of ALN on bone-resorbing cells, bone-forming cells, and net bone volume in the tooth replantation model.

DC and GO prevented inhibition of Rap1A prenylation by ALN *in vitro*

It has been proposed that N-BPs enhance osteogenic differentiation through inhibition of protein prenylation (Chaplet *et al.* 2004, Duque *et al.* 2011) or through activating ERK and JNK (Fu *et al.* 2008). To examine whether endocytic incorporation of ALN is involved in inhibition of small GTPase prenylation, we performed western blot analysis for cell lysates of ROS 17/2.8 cells after treatment with ALN in the presence or absence of DC or GO for 24 h. We detected the unprenylated form of Rap1A markedly at 10^{-4} M ALN, but to a lesser extent at 10^{-6} and 10^{-5} M (Fig. 9A). Co-treatment with 100 μ M DC or 20 μ M GO prevented the accumulation of unprenylated Rap1A by ALN, suggesting that endocytic incorporation of ALN links to the inhibition of small GTPase prenylation *in vitro* by ALN.

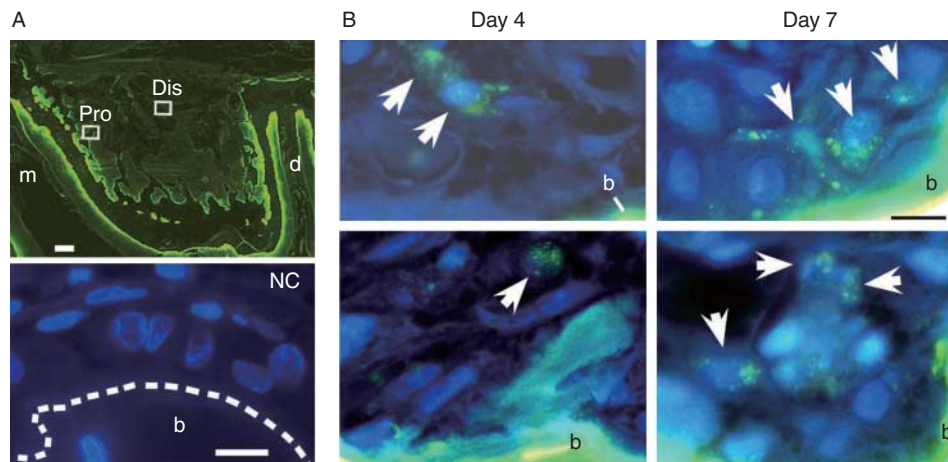


Figure 5

Fluorescence-labeled ALN (F-ALN) is taken into bone-forming cells *in vivo*. (A, Upper panel) Undemineralized longitudinal section of replanted teeth pretreated with F-ALN showing observation sites, proximal (Pro) and distal (Dis) sites for (B), 4 days after replantation. m, mesial root; d, distal root. Scale, 0.2 mm. (Lower panel) Negative control (NC). Sections were obtained from replanted teeth pretreated with non-labeled ALN, 4 days after replantation. No fluorescence was detected on bone surfaces (as indicated by the dotted line) and in cells under the same exposure time as in sections

from replanted teeth pretreated with labeled ALN. Scale bar, 10 μ m.

(B) Incorporation of F-ALN by bone-forming cells adjacent to bone surfaces in bone marrows around replanted teeth (approximate sites indicated by white square Pro in (A); upper panels) and those in bone marrows distant from replanted teeth (approximate sites indicated by white square Dis in (A); lower panels) on days 4 and 7. Arrows indicate mononuclear cells incorporating F-ALN. b, trabecular bone. Scale bar, 10 μ m. Sections were counterstained with DAPI and observed by fluorescence microscopy.

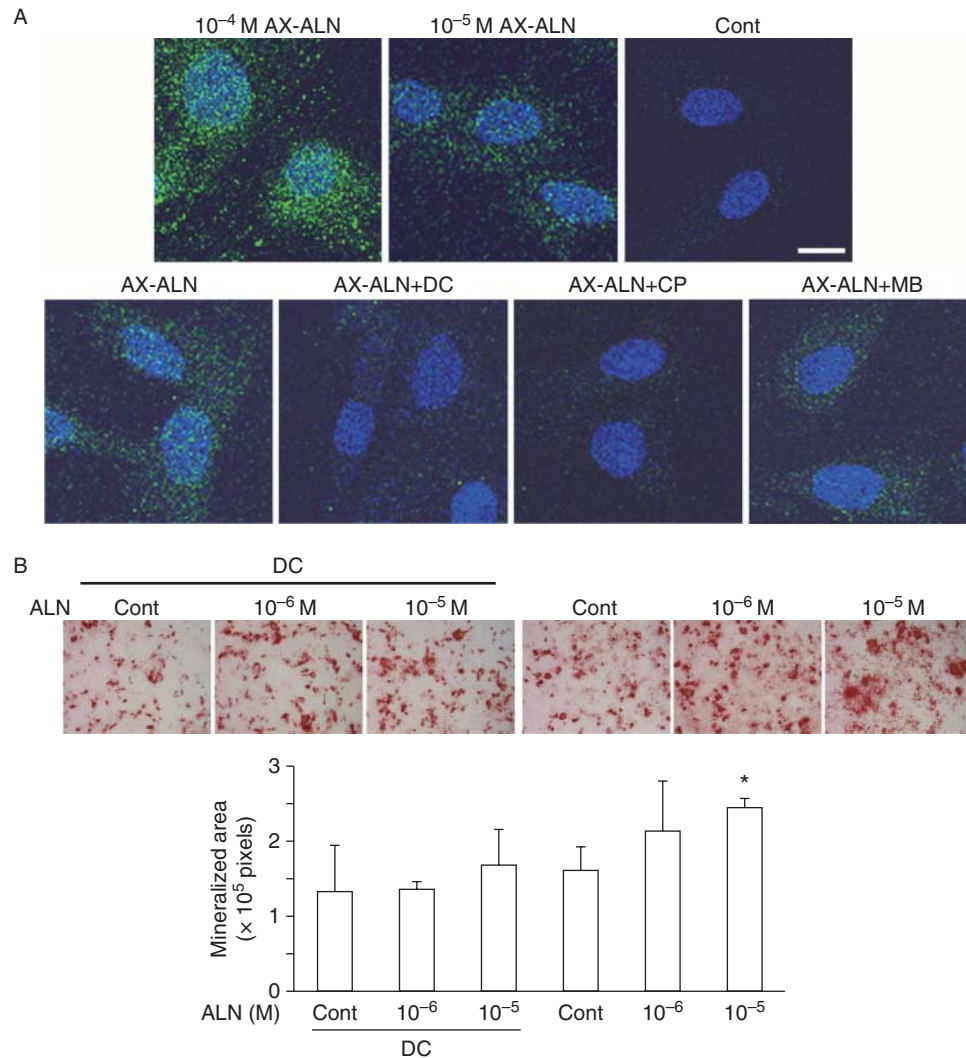
We further tested whether endocytic incorporation of ALN is involved in ERK activation. ALN concentrations of 10^{-6} or 10^{-5} M induced a rapid and transient phosphorylation of ERK1/2 in a dose-dependent manner (Fig. 9B). However, 100 μ M DC did not prevent the ALN-induced phosphorylation of ERKs, suggesting that endocytic incorporation of ALN does not link to the phosphorylation of ERKs.

Discussion

This study indicates that locally applied ALN promotes bone formation by stimulating proliferation and differentiation of bone-forming cells as well as inhibiting osteoclast function. Tracking of F-ALN demonstrated that ALN was taken into cells at bone surfaces of bone marrows in the replanted teeth and into osteoblastic cells *in vitro*. We further demonstrated that local ALN treatment enhanced proliferation and differentiation of bone-forming cells adjacent to the bone surfaces in our *in vivo* model.

Several reports have shown that N-BPs can directly affect osteoblast proliferation and differentiation. Treatment with ALN and zoledronate upregulated osteogenic gene expression in Saos2 osteosarcoma cells (Chaplet *et al.* 2004), human bone-derived cells (Pan *et al.* 2004), and rodent bone marrow stromal cells (Fu *et al.* 2008). ALP activity and osteocalcin production were enhanced by

zoledronate in human osteoblasts from bone biopsies of healthy subjects (Ebert *et al.* 2009, Corrado *et al.* 2010). Mineralization was increased by zoledronate in human bone or bone marrow-derived cells (Pan *et al.* 2004, Ebert *et al.* 2009) and ALN in human mesenchymal stem cells (Duque & Rivas 2007). Here, we found that 3-day treatment of rat calvarial osteoblastic cells with ALN (10^{-6} or 10^{-5} M) at an early differentiation stage induced upregulation of osteocalcin expression and mineralization at a later differentiation stage. By contrast, treatment with a higher ALN concentration, 10^{-4} M, caused deleterious effects with decreased cell viability and the inhibition of cell differentiation, which are consistent with results from previous studies (Idris *et al.* 2008, Orriss *et al.* 2009). Concentrations of ALN released from the ALN-coated implants were estimated to be lower than 10^{-5} M adjacent to the implant surface *in vitro* (Tanzer *et al.* 2005, Gao *et al.* 2009). Similar concentrations (10^{-6} M) could be achieved in the circulation after a short-term intravenous infusion of zoledronate (Ebert *et al.* 2009). Once-yearly treatment with zoledronate for three years leads to increased trabecular bone volume and MAR in women with postmenopausal osteoporosis (Recker *et al.* 2008). Therefore, short-term i.v. infusion as well as short-term local application of N-BP may provide favorable concentrations and promote the differentiation and proliferation of bone-forming cells.

**Figure 6**

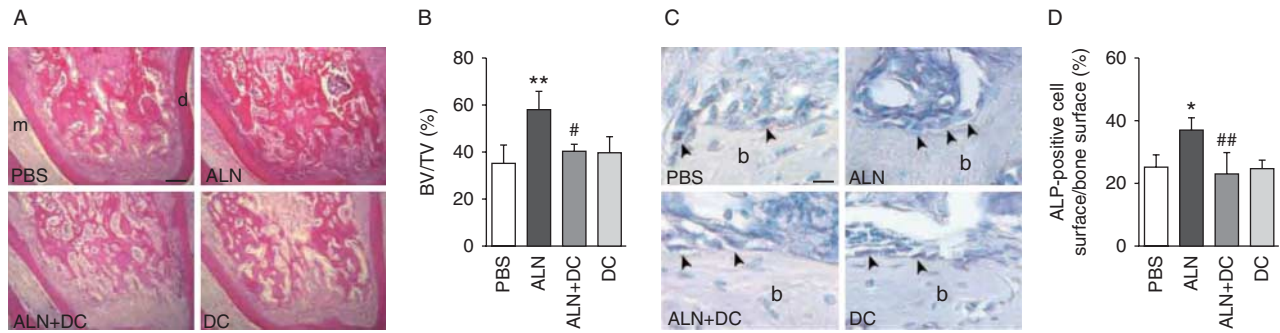
Fluorescence-labeled ALN is taken into bone-forming cells through endocytosis. (A) Cellular uptake of AX-ALN by primary rat osteoblastic cells as observed by confocal laser scanning microscopy. (Upper panels) Cells were incubated with 10^{-4} M AX-ALN, 10^{-5} M AX-ALN, or without AX-ALN (cont) for 4 h at 37 °C. (Lower panels) Effects of endocytosis inhibitors, dansylcadaverine (DC), chlorpromazine (CP), and methyl- β -cyclodextrin (MB) on AX-ALN cellular uptake. Cells were incubated with 10^{-5} M AX-ALN in the absence

(AX-ALN) or presence of 100 μ M DC (AX-ALN+DC), 20 μ M CP (AX-ALN+CP), or 1 mM MB (AX-ALN+MB) for 4 h at 37 °C. Sections were counterstained with DAPI. Scale bar, 10 μ m. (B) Effect of DC on ALN-induced increase in mineralization in calvarial osteoblastic cell culture. (Upper panels) Alizarin red staining at day 21. (Lower panels) Quantification of Alizarin red-stained nodule areas (mineralized area). Each column+bar represents the mean \pm 1 s.d. Significant difference from the control (cont): * P <0.05.

In this study, proliferation and ALP activity of calvarial osteoblasts did not increase after pulse treatment with 10^{-6} and 10^{-5} M ALN *in vitro*, whereas BrdU uptake and ALP activity were increased in cells adjacent to bone surfaces *in vivo*. Previous studies reported that *in vitro* continuous treatment of bone marrow cells with 10^{-8} – 10^{-5} M ALN increased ALP activity (Fu *et al.* 2008) and that treatment with 10^{-13} – 10^{-8} M ALN increased cell proliferation (Giuliani *et al.* 1998). It has also been reported that bone marrow stromal cells from human mandibles are more

susceptible to pamidronate than those from iliac crest based on decreased cell survival and lower ALP activity (Stefanik *et al.* 2008). It is possible that the effects of ALN on ALP activity and cell proliferation in osteoblastic cells may differ depending on the cell stage of bone-forming cells, origins of osteoblastic cells, concentrations of BPs, and duration of treatment time.

Here we found that mononuclear cells including bone marrow stromal cells and/or bone-forming cells took up ALN *in vivo*, and that primary osteoblastic cells

**Figure 7**

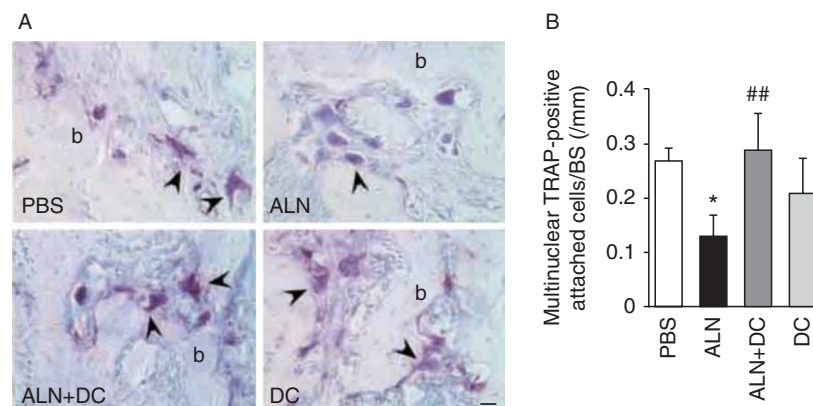
Effect of an endocytosis inhibitor DC on the ALN-induced bone formation *in vivo*. Replanted teeth pretreated with PBS, ALN (1 mM), ALN+DC (1 mM), or DC (1 mM) were dissected on day 7 after tooth replantation. (A) Hematoxylin and eosin staining. m, mesial root; d, distal root. Scale bar, 0.2 mm. (B) Bone volume (BV)/tissue volume (TV) between the mesial and distal roots of replanted teeth was determined. (C) ALP staining. Pictures

were taken from the bone marrow region between the two roots of the replanted teeth. Arrowheads indicate ALP-positive cells on bone surfaces. b, bone. Scale bar, 20 μ m. (D) ALP-positive cell surface/bone surface (%). Significant differences from the PBS group: ** $P < 0.01$ and * $P < 0.05$. Significant differences from the ALN group: ## $P < 0.01$ and # $P < 0.05$.

incorporated ALN *in vitro*, whose incorporation was inhibited by the endocytosis inhibitor DC. In addition, DC prevented the ALN-induced increase of osteocalcin expression *in vitro* and the ALN-induced increases of bone mass and ALP-positive cells *in vivo* by blocking the endocytic incorporation of ALN. There are two possibilities regarding the inhibition of ALN uptake *in vivo* by DC. One possibility is that DC inhibited the cellular uptake of ALN at an early stage after replantation based on our observation that brief exposure to DC inhibited the uptake of F-ALN by osteoblasts *in vitro* (Fig. 6). Another possibility is that DC inhibited the cellular uptake of ALN following desorption of the ALN from the mineralized surfaces over

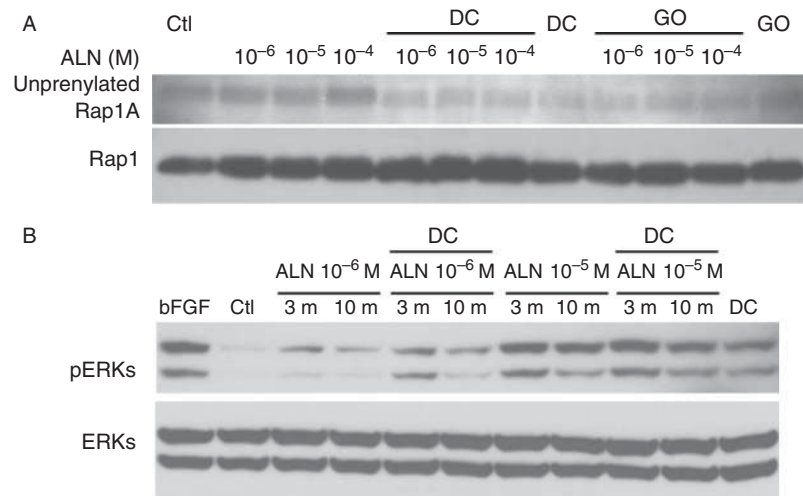
the whole 7 days since osteoblastic cells incorporated N-BP released from dentin slices (Coxon *et al.* 2008). Further investigation would be needed to elucidate the mechanisms of inhibition of endocytosis *in vivo* by DC. Taken together, our findings suggest that endocytic uptake of N-BPs is indispensable for N-BP promotion of bone formation.

We used several inhibitors that interfere selectively with either clathrin-dependent or caveolin-mediated endocytosis (Haigler *et al.* 1980, Chen *et al.* 2009, Kelley *et al.* 2009) to determine the relative importance of these mechanisms for the internalization of N-BPs (Fig. 6A). DC arrests the endocytosis process at the clathrin-coated pit

**Figure 8**

Effect of an endocytosis inhibitor DC on TRAP-positive cells in ALN-treated bone. Replanted teeth pretreated with PBS, ALN (1 mM) ALN+DC (1 mM), or DC (mM) were dissected on day 7 after tooth replantation. (A) TRAP staining. Pictures were taken from bone marrows between the two roots of the replanted teeth. Arrowheads indicate multinuclear TRAP-positive cells

attached to bone surfaces. b, bone. Scale bar, 20 μ m. (B) Numbers of multinuclear TRAP-positive attached cells between the two roots per bone surface (BS (mm)). Significant differences from the PBS group: * $P < 0.05$. Significant differences from the ALN group: ## $P < 0.01$.

**Figure 9**

(A) Endocytosis inhibitor DC prevents the inhibition of Rap1A prenylation by ALN. ROS 17/2.8 cells were treated with or without ALN at the indicated concentrations in the presence or absence of DC (100 μ M) or geranylgeraniol (GO, 20 μ M) for 24 h. Immunoblot analyses were performed for unprenylated Rap1A and Rap1. (B) DC does not affect ALN-induced phosphorylation of ERK. ROS 17/2.8 cells were treated with ALN

(10^{-6} or 10^{-5} M) for 3 min (3 m) or 10 min (10 m) in the presence or absence of DC (100 μ M) or with DC (100 μ M) only for 10 min. Cells were also treated with or without bFGF (10 ng/ml) for 15 min as positive control or negative control (Ct). Immunoblot analyses were performed for phosphorylated ERK and total ERK.

stage (Chen *et al.* 2009). Another inhibitor, CP induces a loss of clathrin-coated pits from the cell surface (Ivanov 2008), while MB inhibits a caveolae-like endocytosis (Ivanov 2008). Since DC and CP, but not MB, suppressed ALN incorporation in this study, we suggest that osteoblastic cells may incorporate N-BPs through clathrin-mediated endocytic pathways. In a previous study on endocytosis of fluorescently labeled N-BPs by macrophages and osteoclasts (Thompson *et al.* 2006), the authors observed that intracellular uptake of the labeled N-BPs was inhibited by DC and colocalized with dextran but not with markers of adsorptive (wheat germ agglutinin) or receptor-mediated (transferrin) endocytosis. The role of intracellular uptake pathways in osteoblastic cells in this study seems to be similar to those in the macrophages and osteoclasts.

Regarding the mechanisms of BP effects on osteoblastic function, several reports suggest the involvement of inhibition of small GTPase prenylation. Pitavastatin and zoledronate enhance expression of bone-related genes by inhibition of Rho GTPase in human osteoblastic cells and osteosarcoma Saos2 cells (Ohnaka *et al.* 2001, Chaplet *et al.* 2004). Geranylgeranyl-pyrophosphate synthase is down-regulated during osteoblastic differentiation in MC3T3-E1 (Yoshida *et al.* 2006). Recently, it has been reported that treatment with 10^{-8} M ALN or 5 μ M GGTI-298, geranylgeranyltransferase inhibitor, increases osteocalcin

expression, mineralization, and unprenylated Rap1 in human mesenchymal stem cells (Duque *et al.* 2011). In this study, addition of GO prevented the ALN-induced upregulation of osteocalcin in calvarial osteoblastic cells. We further detected the unprenylated form of Rap1A following treatment of ROS 17/2.8 cells with ALN, which was reduced by endocytosis inhibitor DC or GO. The present findings suggest that N-BP stimulates osteoblast differentiation through endocytic incorporation of N-BP, which subsequently inhibits small GTPase prenylation.

Some studies have proposed an extracellular mechanism of BP action and an involvement of intracellular signaling in N-BP induced osteoblastic differentiation (Mathov *et al.* 2001, Fu *et al.* 2008, Bellido & Plotkin 2011). Prevention of osteoblast and osteocyte apoptosis by BPs (10^{-9} – 10^{-6} M) is mediated by connexin 43 hemichannel opening and activation of Src and ERKs (Mathov *et al.* 2001, Bellido & Plotkin 2011). The ALN-induced upregulation of osteogenic markers in bone marrow stromal cells is possibly due to the activation of ERK and JNK (Fu *et al.* 2008). Here we detected an increase in ALN-induced phosphorylation of ERKs, which was not blocked by the addition of endocytosis inhibitor DC. Thus, the ALN-induced phosphorylation of ERKs may be mediated mainly through an extracellular mechanism, but not through direct incorporation of ALN. Therefore, we suggest that bone formation by direct incorporation of

ALN may be mediated through inhibition of the mevalonate pathway rather than activation of the ERK pathway. Further investigation is needed to explore the molecular targets and downstream pathways for the anabolic effects of N-BPs.

N-BPs have been used to treat systemic bone metabolic disorders. This and earlier (Wilkinson & Little 2011) studies further add a possibility that local application of N-BPs may be useful for local bone augmentation. It has been reported that locally administered ALN increased bone mineral density in a rabbit model (Omi *et al.* 2007). Surface coatings of zoledronate and pamidronate have also been reported to cause bone increase around orthopedic implants in animal models (Tanzer *et al.* 2005, Wermelin *et al.* 2008, Gao *et al.* 2009). Local delivery of N-BPs is a reasonable approach because it reduces the amount of drug used and preferentially targets the site of interest, thereby avoiding systemic exposure and adverse side effects (Bobynd *et al.* 2009). A recent clinical trial of dental implants coated with N-BP has suggested that the use of local N-BP release might be a promising principle (Abtahi *et al.* 2012). Our results would further provide mechanistic bases for local effects by N-BPs.

Supplementary data

This is linked to the online version of the paper at <http://dx.doi.org/10.1530/JOE-13-0040>.

Declaration of interest

The authors declare that there is no conflict of interest that could be perceived as prejudicing the impartiality of the research reported.

Funding

This work was supported by grants from Japanese MEXT.HAITEKU (2005–2009, H050151) and from the Ministry of Education, Science and Culture of Japan (21659425 and 19390475).

References

- Abtahi J, Tengvall P & Aspenberg P 2012 A bisphosphonate-coating improves the fixation of metal implants in human bone. A randomized trial of dental implants. *Bone* **50** 1148–1151. (doi:10.1016/j.bone.2012.02.001)
- Azuma Y, Sato H, Oue Y, Okabe K, Ohta T, Tsuchimoto M & Kiyoki M 1995 Alendronate distributed on bone surfaces inhibits osteoclastic bone resorption *in vitro* and in experimental hypercalcemia models. *Bone* **16** 235–245. (doi:10.1016/8756-3282(94)00035-X)
- Bellido T & Plotkin LI 2011 Novel actions of bisphosphonates in bone: preservation of osteoblast and osteocyte viability. *Bone* **49** 50–55. (doi:10.1016/j.bone.2010.08.008)
- Bobynd JD, McKenzie K, Karabasz D, Krygier JJ & Tanzer M 2009 Locally delivered bisphosphonate for enhancement of bone formation and implant fixation. *Journal of Bone and Joint Surgery* **91** 23–31. (doi:10.2106/JBJS.I.00518)
- Chaplet M, Detry C, Deroanane C, Fisher LW & Castronovo V 2004 Zoledronic acid up-regulates bone sialoprotein expression in osteoblastic cells through Rho GTPase inhibition. *Biochemical Journal* **384** 591–598. (doi:10.1042/BJ20040380)
- Chen CL, Hou WH, Liu IH, Hsiao G, Huang SS & Huang JS 2009 Inhibitors of clathrin-dependent endocytosis enhance TGF β signaling and responses. *Journal of Cell Science* **122** 1863–1871. (doi:10.1242/jcs.038729)
- Corrado A, Neve A, Maruotti N, Gaudio A, Marucci A & Cantatore FP 2010 Dose-dependent metabolic effect of zoledronate on primary human osteoblastic cell cultures. *Clinical and Experimental Rheumatology* **28** 873–879.
- Coxon FP, Thompson K, Roelofs AJ, Ebetino FH & Rogers MJ 2008 Visualizing mineral binding and uptake of bisphosphonate by osteoclasts and non-resorbing cells. *Bone* **42** 848–860. (doi:10.1016/j.bone.2007.12.225)
- Dunford JE, Rogers MJ, Ebetino FH, Phipps RJ & Coxon FP 2006 Inhibition of protein prenylation by bisphosphonates causes sustained activation of Rac, Cdc42, and Rho GTPases. *Journal of Bone and Mineral Research* **21** 684–694. (doi:10.1359/jbmr.060118)
- Duque G & Rivas D 2007 Alendronate has an anabolic effect on bone through the differentiation of mesenchymal stem cells. *Journal of Bone and Mineral Research* **22** 1603–1611. (doi:10.1359/jbmr.070701)
- Duque G, Vidal C & Rivas D 2011 Protein isoprenylation regulates osteogenic differentiation of mesenchymal stem cells: effect of alendronate, and farnesyl and geranylgeranyl transferase inhibitors. *British Journal of Pharmacology* **162** 1109–1118. (doi:10.1111/j.1476-5381.2010.01111.x)
- Ebert R, Zeck S, Krug R, Meissner-Weigl J, Schneider D, Seefried L, Eulert J & Jakob F 2009 Pulse treatment with zoledronic acid causes sustained commitment of bone marrow derived mesenchymal stem cells for osteogenic differentiation. *Bone* **44** 858–864. (doi:10.1016/j.bone.2009.01.009)
- Fu L, Tang T, Miao Y, Zhang S, Qu Z & Dai K 2008 Stimulation of osteogenic differentiation and inhibition of adipogenic differentiation in bone marrow stromal cells by alendronate via ERK and JNK activation. *Bone* **43** 40–47. (doi:10.1016/j.bone.2008.03.008)
- Gao Y, Luo E, Hu J, Xue J, Zhu S & Li J 2009 Effect of combined local treatment with zoledronic acid and basic fibroblast growth factor on implant fixation in ovariectomized rats. *Bone* **44** 225–232. (doi:10.1016/j.bone.2008.10.054)
- Giuliani N, Pedrazzoni M, Negri G, Passeri G, Impicciatore M & Girasole G 1998 Bisphosphonates stimulate formation of osteoblast precursors and mineralized nodules in murine and human bone marrow cultures *in vitro* and promote early osteoblastogenesis in young and aged mice *in vivo*. *Bone* **22** 455–461. (doi:10.1016/S8756-3282(98)00033-7)
- Haigler HT, Maxfield FR, Willingham MC & Pastan I 1980 Dansylcadaverine inhibits internalization of 125I-epidermal growth factor in BALB 3T3 cells. *Journal of Biological Chemistry* **255** 1239–1241.
- Ideno H, Takanabe R, Shimada A, Imaizumi K, Araki R, Abe M & Nifuji A 2009 Protein related to DAN and cerberus (PRDC) inhibits osteoblastic differentiation and its suppression promotes osteogenesis *in vitro*. *Experimental Cell Research* **315** 474–484. (doi:10.1016/j.yexcr.2008.11.019)
- Idris AI, Rojas J, Greig IR, Van't Hof RJ & Ralston SH 2008 Amino-bisphosphonates cause osteoblast apoptosis and inhibit bone nodule formation *in vitro*. *Calcified Tissue International* **82** 191–201. (doi:10.1007/s00223-008-9104-y)
- Ivanov AI 2008 Pharmacological inhibition of endocytic pathways: is it specific enough to be useful?. In *Exocytosis and Endocytosis*, pp 15–33. Ed. AI Ivanov. Totowa, NJ: Human Press.

- Kelley R, Ren R, Pi X, Wu Y, Moreno I, Willis M, Moser M, Ross M, Podkova M, Attisano L *et al.* 2009 A concentration-dependent endocytic trap and sink mechanism converts Bmper from an activator to an inhibitor of Bmp signaling. *Journal of Cell Biology* **184** 597–609. (doi:10.1083/jcb.200808064)
- Komatsu K, Shimada A, Shibata T, Shimoda S, Oida S, Kawasaki K & Nifuji A 2008 Long-term effects of local pretreatment with alendronate on healing of replanted rat teeth. *Journal of Periodontal Research* **43** 194–200. (doi:10.1111/j.1600-0765.2007.01012.x)
- Luckman SP, Hughes DE, Coxon FP, Graham R, Russell G & Rogers MJ 1998 Nitrogen-containing bisphosphonates inhibit the mevalonate pathway and prevent post-translational prenylation of GTP-binding proteins, including Ras. *Journal of Bone and Mineral Research* **13** 581–589. (doi:10.1359/jbmr.1998.13.4.581)
- Masaïke Y, Takagi T, Hirota M, Yamada J, Ishihara S, Yung TM, Inoue T, Sawa C, Sagara H, Sakamoto S *et al.* 2010 Identification of dynamin-2-mediated endocytosis as a new target of osteoporosis drugs, bisphosphonates. *Molecular Pharmacology* **77** 262–269. (doi:10.1124/mol.109.059006)
- Masarachia P, Weinreb M, Balena R & Rodan GA 1996 Comparison of the distribution of ³H-alendronate and ³H-etidronate in rat and mouse bones. *Bone* **19** 281–290. (doi:10.1016/8756-3282(96)00182-2)
- Mathov I, Plotkin LI, Sgarlata CL, Leoni J & Bellido T 2001 Extracellular signal-regulated kinases and calcium channels are involved in the proliferative effect of bisphosphonates on osteoblastic cells *in vitro*. *Journal of Bone and Mineral Research* **16** 2050–2056. (doi:10.1359/jbmr.2001.16.11.2050)
- Ohnaka K, Shimoda S, Nawata H, Shimokawa H, Kaibuchi K, Iwamoto Y & Takayanagi R 2001 Pitavastatin enhanced BMP-2 and osteocalcin expression by inhibition of Rho-associated kinase in human osteoblasts. *Biochemical and Biophysical Research Communications* **287** 337–342. (doi:10.1006/bbrc.2001.5597)
- Omi H, Kusumi T, Kijima H & Toh S 2007 Locally administered low-dose alendronate increases bone mineral density during distraction osteogenesis in a rabbit model. *Journal of Bone and Joint Surgery* **89** 984–988. (doi:10.1302/0301-620X.89B7.18980)
- Orriss IR, Key ML, Colston KW & Arnett TR 2009 Inhibition of osteoblast function *in vitro* by aminobisphosphonates. *Journal of Cellular Biochemistry* **106** 109–118. (doi:10.1002/jcb.21983)
- Pan B, To LB, Farrugia AN, Findlay DM, Green J, Gronthos S, Evdokiou A, Lynch K, Atkins GJ & Zannettino ACW 2004 The nitrogen-containing bisphosphonate, zoledronic acid, increases mineralisation of human bone-derived cells *in vitro*. *Bone* **34** 112–123. (doi:10.1016/j.bone.2003.08.013)
- Parfitt AM, Drezner MK, Glorieux FH, Kanis JA, Malluche H, Meunier PJ, Ott SM & Recker RR 1987 Bone histomorphometry: standardization of nomenclature, symbols, and units. *Journal of Bone and Mineral Research* **2** 595–610. (doi:10.1002/jbmr.5650020617)
- Recker R, Delmas PD, Halse J, Reid IR, Boonen S, García-Hernandez PA, Supronik J, Lewiecki EM, Ochoa L, Miller P *et al.* 2008 Effects of intravenous zoledronic acid once yearly on bone remodeling and bone structure. *Journal of Bone and Mineral Research* **23** 6–16. (doi:10.1359/jbmr.070906)
- Reinholtz GG, Getz B, Pederson L, Sanders ES, Subramaniam M, Ingle JN & Spelsberg TN 2000 Bisphosphonates directly regulate cell proliferation, differentiation, and gene expression in human osteoblasts. *Cancer Research* **60** 6001–6007.
- Reszka AA, Halasy-Nagy J & Rodan GA 2001 Nitrogen-bisphosphonates block retinoblastoma phosphorylation and cell growth by inhibiting the cholesterol biosynthetic pathway in a keratinocyte model for esophageal irritation. *Molecular Pharmacology* **59** 193–202. (doi:10.1124/mol.59.2.193)
- Roelofs AJ, Coxon FP, Ebetino FH, Lundy MW, Henneman ZJ, Nancollas GH, Sun S, Blazewska KM, Bala JL, Kashemirov BA *et al.* 2010 Fluorescent risedronate analogues reveal bisphosphonate uptake by bone marrow monocytes and localization around osteocytes *in vivo*. *Journal of Bone and Mineral Research* **25** 606–616. (doi:10.1359/jbmr.091009)
- Rogers MJ, Crockett JC, Coxon FP & Monkkonen J 2011 Biochemical and molecular mechanisms of action of bisphosphonates. *Bone* **49** 34–41. (doi:10.1016/j.bone.2010.11.008)
- Sato M, Grasser W, Endo N, Akins R, Simmons H, Thompson DD, Golub E & Rodan G 1991 Bisphosphonate action: alendronate localization in rat bone and effects on osteoclast ultrastructure. *Journal of Clinical Investigation* **88** 2095–2105. (doi:10.1172/JCI115539)
- Schenk RK, Olah AJ & Herrmann W 1984 Preparation of calcified tissues for light microscopy. In *Methods of Calcified Tissue Preparation*, pp 1–56. Ed. GR Dickson. Amsterdam: Elsevier.
- Shibata T, Komatsu K, Shimada A, Shimoda S, Oida S, Kawasaki K & Chiba M 2004 Effects of alendronate on restoration of biomechanical properties of periodontium in replanted rat molars. *Journal of Periodontal Research* **39** 405–414. (doi:10.1111/j.1600-0765.2004.00755.x)
- Stefanik D, Sarin J, Lam T, Levin L, Leboy PS & Akintoye SO 2008 Disparate osteogenic response of mandible and iliac crest bone marrow stromal cells to pamidronate. *Oral Diseases* **14** 465–471. (doi:10.1111/j.1601-0825.2007.01402.x)
- Tanzer M, Karabasz D, Krygier JJ, Cohen R & Bobyn JD 2005 Bone augmentation around and within porous implants by local bisphosphonates elution. *Clinical Orthopaedics and Related Research* **441** 30–39. (doi:10.1097/01.blo.0000194728.62996.2d)
- Thompson K, Rogers MJ, Coxon FP & Crockett JC 2006 Cytosolic entry of bisphosphonate drugs requires acidification of vesicles after fluid-phase endocytosis. *Molecular Pharmacology* **69** 1624–1632. (doi:10.1124/mol.105.020776)
- Wada Y, Kataoka H, Yokose S, Ishizuya T, Miyazono K, Gao Y-H, Shibasaki Y & Yamaguchi A 1998 Changes in osteoblasts phenotype during differentiation of enzymatically isolated rat calvarial cells. *Bone* **22** 479–485. (doi:10.1016/S8756-3282(98)00039-8)
- Wermelin K, Suska F, Tengvall P, Thomsen P & Aspenberg P 2008 Stainless steel screws coated with bisphosphonates gave stronger fixation and more surrounding bone. Histomorphometry in rats. *Bone* **42** 365–371. (doi:10.1016/j.bone.2007.10.013)
- Wilkinson JM & Little DG 2011 Bisphosphonates in orthopedic applications. *Bone* **49** 95–102. (doi:10.1016/j.bone.2011.01.009)
- Yoshida T, Asanuma M, Grossman L, Fuse M, Shibata T, Yonekawa T, Tanaka T, Ueno K, Yasuda T, Saito Y *et al.* 2006 Geranylgeranylpyrophosphate (GGPP) synthase is down-regulated during differentiation of osteoblastic cell line MC3T3-E1. *FEBS Letters* **580** 5203–5207. (doi:10.1016/j.febslet.2006.08.060)
- Zaheer A, Lenkinski RE, Mahmood A, Jones AG, Cantley LC & Frangioni JV 2001 *In vivo* near-infrared fluorescence imaging of osteoblastic activity. *Nature Biotechnology* **19** 1148–1154. (doi:10.1038/nbt1201-1148)

Received in final form 14 August 2013

Accepted 19 August 2013